Fluctuations associated with a filamentary density depletion

J. E. Maggs[a] and G. J. Morales
Department of Physics and Astronomy, University of California, Los Angeles, Los Angeles, California 90095

(Received 2 August 1996; accepted 21 October 1996)

Density and magnetic fluctuations arising spontaneously in a narrow field-aligned density striation in a magnetized discharge He plasma are found to exhibit a radial eigenmode structure. The nature of the fluctuations depends upon the electron plasma beta, β_e. For β_e greater than the electron to ion mass ratio ($\beta_e > m/M$) the frequency spectrum exhibits sharply peaked eigenfrequencies with the density and magnetic fluctuations strongly coupled so that the growing mode is identified as the drift-Alfvén wave. For β_e less than the mass ratio ($\beta_e < m/M$) the density and magnetic fluctuations separate in frequency and broadband magnetic shear Alfvén wave turbulence develops. The driving source for the fluctuations is the cross-field density and temperature gradients in the edge of the striation which have scale lengths on the order of the electron skin depth. The fluctuations associated with the striation are compared to the edge fluctuations of the plasma column which are found to exhibit a universal exponential frequency spectrum. © *1997 American Institute of Physics.* [S1070-664X(97)00102-X]

I. INTRODUCTION

It is becoming more apparent that microscopic filamentary structures[1–4] are a fundamental feature of magnetized plasmas that are far from thermal equilibrium. Magnetic field-aligned filamentary structures can consist of density depletions or enhancements, localized pressure changes, current channels, charged flux tubes, or combinations thereof, depending upon the specific boundary conditions and sources that drive the plasma away from thermal equilibrium. By microscopic it is meant that the scale length across the confining magnetic field is comparable to the larger of the two key physical parameters, the electron skin depth, c/ω_{pe} (where c is the speed of light and ω_{pe} the electron plasma frequency) or the ion Larmor radius ρ_i.

Observational evidence for microscopic filamentary structures has been obtained over a wide range of plasma environments including tokamak experiments,[5–7] ionospheric modification studies,[8] *in situ* measurements of the auroral ionosphere by rockets[9] and spacecraft.[10] Remote imaging of the solar corona and the intergalactic medium has also identified filamentary structures. Of course, filaments can develop in the propagation of intense laser beams through plasmas, and applications of narrow plasma waveguides[11] are of current interest. While there are many important and interesting features associated with a basic filament (i.e., a microscopic plasma) embedded in a larger plasma, such as its shape, lifetime, and contribution to transport, the present experimental study focuses on the role of a magnetic field-aligned density depletion (also referred to as a ''striation'') as a generator of low frequency fluctuations, i.e., in the frequency range $\omega \approx 0.1$–$0.3\Omega_i$, where Ω_i is the ion gyrofrequency.

These low frequency fluctuations generated in the pressure gradient regions of the striation are of interest because the short transverse scale lengths associated with the striation give rise to Alfvén wave fluctuations with large perpendicular wave number[12,13] (i.e., $k_\perp \geqslant \omega_{pe}/c$) which results in wave electric fields parallel to the confining magnetic field. Such fields can lead to significant parallel electron acceleration as the waves propagate away from the striation. Two cases in which such a process may play an important role are anomalous cross-field electron transport[14,15] in magnetic confinement devices, and formation of fast electron beams responsible for the aurora.[16] Of course, substantial ion heating[17] can also result from the large perpendicular electric field and there is significant interest[18] in the role that such a process plays in the generation of fast ions in the auroral ionosphere.

The present laboratory study investigates the spontaneous fluctuations in density and magnetic field generated by a controlled magnetic field-aligned density depletion whose cross-field scale length is on the order of c/ω_{pe} and much larger than ρ_i. The striation is positioned near the center of a large cylindrical plasma column so that the radial behavior is essentially that of an infinite medium. Axially the striation investigated is approximately ten meters long (corresponding to over 10^6 Debye lengths) which is sufficient for Alfvén wave phenomena to dominate the plasma dynamics. It is found that substantial density and magnetic fluctuations ($\delta n/n_0 \approx 0.2$; $\delta B/B_0 \approx 2\times 10^{-3}$) arise spontaneously along a filamentary density depletion. The fluctuations are trapped within the low density region of the striation with a radial structure having scale sizes on the order of the cross-field gradient length. Density fluctuations can be strongly coupled to shear-like magnetic fluctuations depending upon the electron plasma beta, β_e. At higher values of β_e ($> m/M$, where m is the electron mass and M the ion mass) the fluctuations exhibit a coherent eigenmode structure. At lower values of β_e ($< m/M$) the coherent fluctuations evolve towards broadband Alfvén wave turbulence collimated along the density striation. A detailed examination of the current patterns in the plasma indicates that the cross-field gradients of plasma density and temperature are the driving sources for the fluctuations.

[a]Electronic mail: maggs@physics.ucla.edu

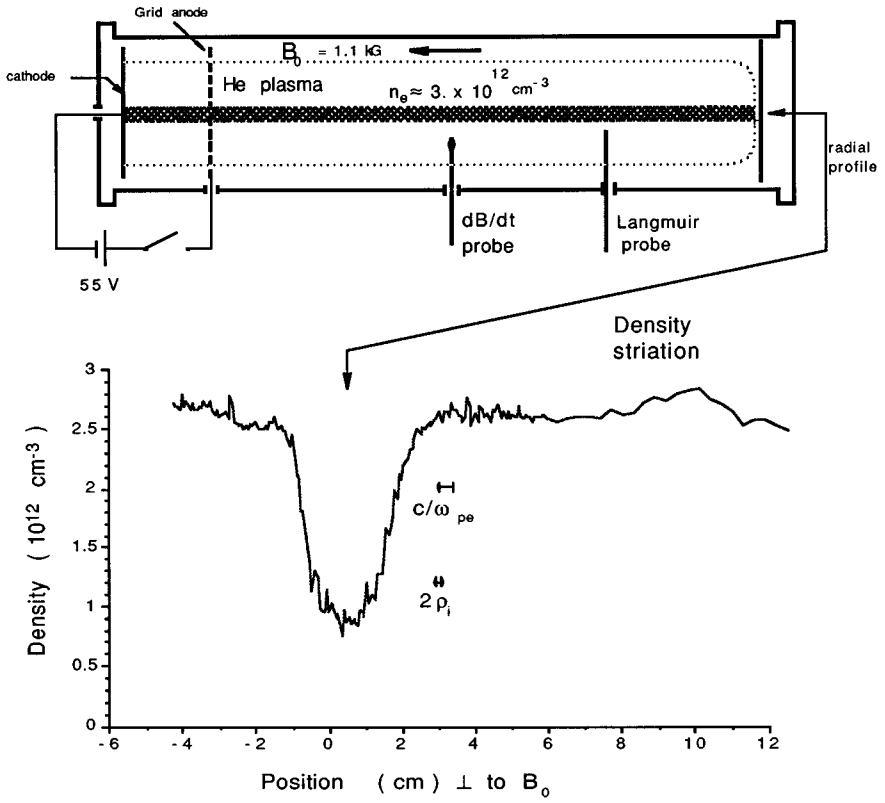

FIG. 1. A schematic representation of the experimental setup. A density striation running the entire length of the machine is created by selective coating or masking of the cathode. A radial density profile in the vicinity of the striation shows the density gradient scale length is on the order of the electron skin depth.

The present study describes, in detail, the experimental findings and uses theoretical results only for the purpose of classifying the different behaviors (e.g., electrostatic drift waves, drift-Alfvén waves, pure Alfvén waves). A separate theoretical study will address the details of the properties of drift waves related to the striation system, and another will consider the Alfvén wave features. The present manuscript is organized as follows. Section II describes the apparatus and the static properties of the striation. The temporal evolution and spatial structure of the fluctuations is presented in Sec. III. Properties of the density and magnetic spectra are given in Sec. IV while a comparison between the behavior of fluctuations observed at the plasma edge and those intrinsic to the narrow filament is presented in Sec. V. Section VI contains a discussion and comparison of the present results with those of previous related experiments.

II. EXPERIMENTAL SETUP

The studies reported here were conducted in the Large Plasma Device[19] (LAPD) at the University of California, Los Angeles. A schematic of the LAPD illustrating the elements used in the formation and study of a controlled striation is shown in Fig. 1. The plasma is generated by electrons (primaries) emitted from a heated, barium oxide coated cathode and subsequently accelerated by a semitransparent (transmission efficiency ≈50%) grid anode located 60 cm from the cathode. The accelerated primaries drift into a 9.4 m long vacuum chamber and strike neutral He gas at a fill pressure of 2×10^{-4} Torr to generate a He^+ plasma with a greater than 75% degree of ionization. For the operating conditions used in these studies axially uniform plasmas 45 cm in diameter are formed with measured plasma densities in the range $n_e \approx 1-4\times10^{12}$ cm^{-3}, $T_e \approx 5-15$ eV, and estimated ion temperature $T_i \approx 0.1-1$ eV. The strength of the axial magnetic field is varied from 0.5 to 2 kG to attain different values of plasma beta, β_e. Discharge currents in the range of 0.3 to 3 kA are used to obtain different radial density profiles. In these experiments the end of the plasma column is terminated by an electrically floating copper plate. Thus there is no net current flowing in the plasma in which the measurements are taken between the grid anode and the copper endplate.

Density striations are generated by two methods. The most ideal method consists of not applying the barium oxide coating to small spot (≈1 cm radius) near the center of the nickel cathode so that primaries are not emitted from this region. Without primaries plasma is not formed along field lines threading the spot and a density depletion results. A drawback of this method is that the position and size of the striation are fixed once the cathode is coated. Changing the striation parameters requires removing and recoating the cathode, a time consuming process. In addition the presence of the striation affects other experiments performed in the plasma. The other method is more flexible. It consists of placing a small copper disk supported on a long thin (≈2 mm diam.) ceramic shaft at a distance of 2–3 cm from a uniformly coated cathode. In this manner emission of primaries is suppressed and a density striation results along the

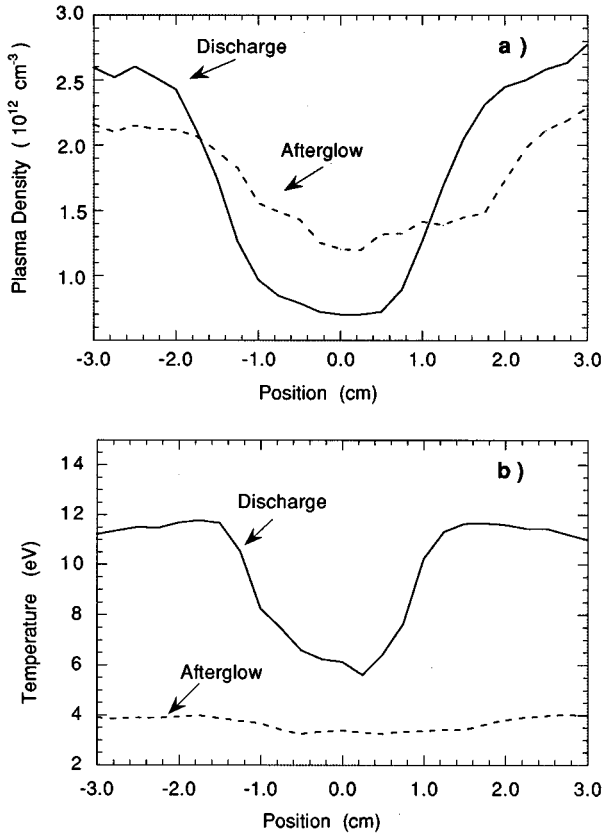

FIG. 2. Radial profiles of plasma density (a) and temperature (b) on a line through the center of the striation during the discharge and 200 μs after the discharge.

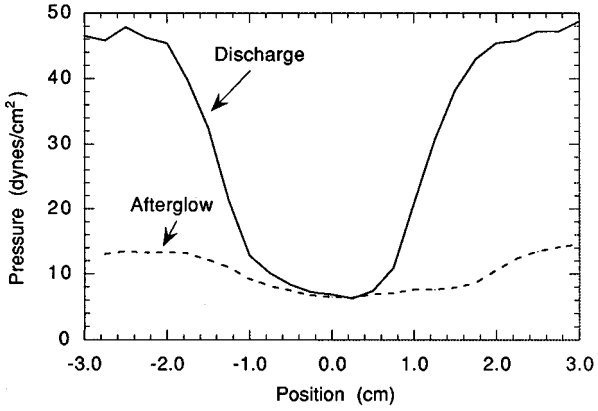

FIG. 3. Pressure profiles in the vicinity of the striation during and after the discharge.

field lines threading the disk. This technique results in density striations with properties nearly identical to those generated with the selective coating method. A drawback to this technique is that the disk support shaft introduces the undesirable feature of breaking the azimuthal symmetry of the striation. However, the properties of magnetic and density fluctuations in striations reported here have been found to be indistinguishable for the two methods of striation formation.

The radial dependence of the plasma density and electron temperature (measured with a small Langmuir probe at an axial location near the middle of the plasma column) in the region around a typical striation are shown in Figs. 2(a) and 2(b), respectively. The two curves shown in each of these figures correspond to conditions while the discharge current is on (primaries are being emitted from the cathode) and in the afterglow, i.e., when the primaries are absent. It should be noted that the spatial region shown in Fig. 2 corresponds to a small sector of the plasma profile whose edges are 20 cm from the center of the striation. For reference, typical parameter values in the plasmas used for these studies are: electron skin depth $c/\omega_{pe} \approx 5$ mm, ion Larmor radius $\rho_i \approx 0.5-2$ mm, and the ion sound gyroradius $\rho_s = (T_e/M)^{1/2}/\Omega_i \approx 2-5$ mm. Hence, the ordering of spatial scales in these studies are $L_n \geqslant L_T \approx c/\omega_{pe} \geqslant \rho_s > \rho_i$, where L_T and L_n are temperature and density scale lengths. It is evident from Fig. 2 that the temperature outside the striation decreases rapidly after the discharge is terminated, while the density decays more slowly since its dynamics are governed mainly by axial flow at the sound speed.

Figure 3 combines the dependencies shown in Fig. 2 to illustrate the pressure profiles during the discharge, when vigorous wave activity is observed, and in the afterglow when wave activity subsides. It is clear that the radial pressure gradient drops by more than a factor of 3 between these two modes of operation.

The dependence of the density profile of the striation on the external control parameters is shown in Fig. 4. For a fixed magnetic field of 1 kG, Fig. 4(a) indicates that plasma density increases with increasing discharge current. The density outside the striation increases approximately linearly while the density at the bottom of the striation responds more slowly. The net result is that discharge current primarily controls the density gradient. Figure 4(b) illustrates that at a fixed, relatively large, discharge current of 2.6 kA the density profile remains insensitive to increases in the magnetic field. The decrease in slope at the edges of the striation is apparently a systematic feature that may be a consequence of the increase in bandwidth of the wave activity as the magnetic field is increased. That is, coherent waves do not cause irreversible changes, but a broad spectrum of waves result in cross-field transport.

Since the wave activity of interest is present while the discharge current is on, it is reasonable to ask if field-aligned currents are responsible for the observed wave growth. To explore this possibility a radial mapping of the axial current is performed with a small (1 mm^2) double-sided Langmuir probe in the region around the striation. To measure the magnetic field-aligned current the probe is oriented so that the normal to each face is parallel (or antiparallel) to the magnetic field. A linear voltage ramp is then applied to both faces simultaneously, sweeping from the ion saturation current regime to the electron saturation current regime. The current at any energy encompassed by the voltage sweep can be found from the current-voltage traces from each face, so that the current carried by any given particle population can be determined. Here, however, we present only the total current. The total field-aligned current is found from the difference in the probe currents to each face when the voltage sweep passes through plasma potential. A radial profile is

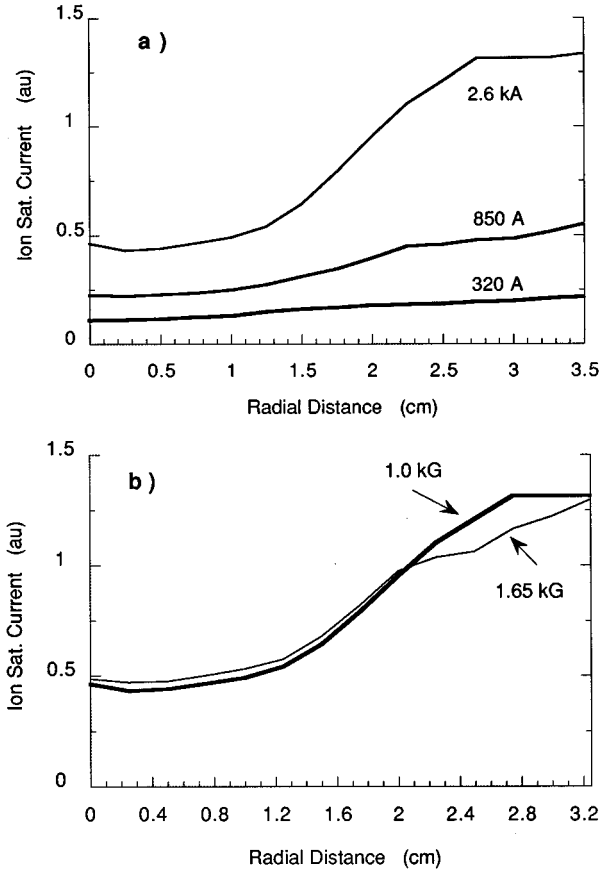

FIG. 4. Changes in the ion saturation current profile of the striation for different discharge currents (a) and different background magnetic field strength (b).

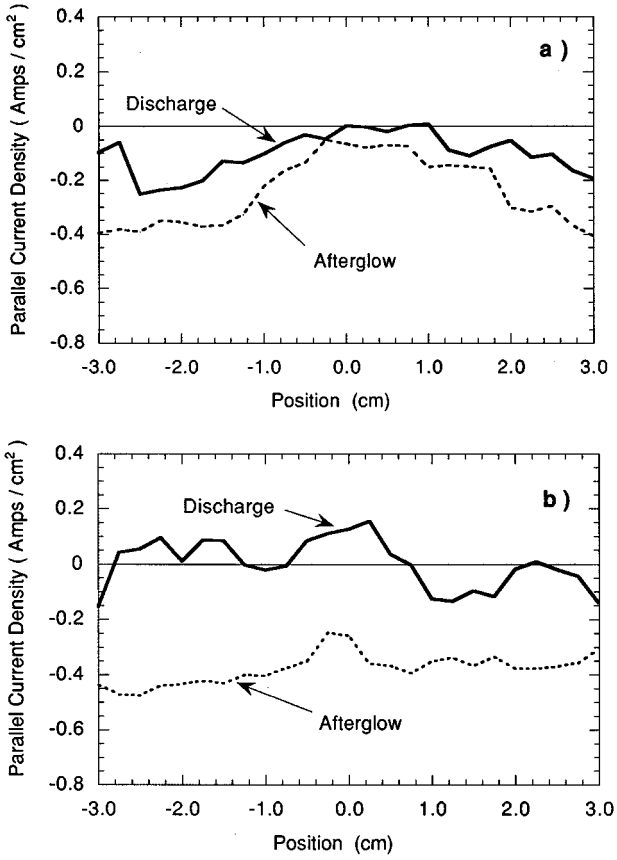

FIG. 5. Radial profiles of the magnetic field-aligned current in the plasma during and after the discharge with a density striation (a) and without a striation (b).

obtained by averaging over 20 shots taken at each individual radial location. The rms deviation from this average gives an indication of the current fluctuations at each radial location.

Figure 5(a) exhibits the current profiles obtained in the presence of the striation while the discharge is on and also in the afterglow. Figure 5(b) shows the equivalent dependencies when the disk forming the striation is removed. Axial currents are carried by two distinct populations. Electrons emitted from the cathode form a fast, tail population along the entire length of the device and carry an electrical current directed towards the cathode. However, in the main body of the plasma column (i.e., the region between the grid anode and copper endplate) the current carried by the fast electrons is canceled by a drift in the bulk electron population. It is important to note that in this region the total current is zero when integrated over the entire cross section of the plasma column and thus may be nonzero on any particular field line. The variation of axial plasma current from field line to field line is apparent in Fig. 5(b), but the average current across the 6 cm section of plasma shown is nearly zero within the accuracy of the measurement. In contrast, in the afterglow there is a net current flowing away from the anode due to the continued drift of the bulk plasma in the absence of any canceling current due to primaries. The current shown in Fig. 5(b) corresponds to a drift of the bulk plasma at about 0.1 the electron thermal speed. The situation is changed in the presence of the striation. As shown in Fig. 5(a), even during the discharge there is a systematic variation to the current profile which mirrors the density profile. In both the afterglow and discharge the current is minimum at the bottom of the striation and largest in the bulk plasma. Again there is a net residual current when the discharge is terminated but the current profile clearly shows the presence of the striation. Although there are clear differences in the axial currents in the absence and presence of the striation, the perspective obtained by examining the radial profiles is that the axial current is not the driving source of the fluctuations. For example, in the presence of the striation a nonzero axial current does indeed flow in the gradient region of the striation where the fluctuations are present during the discharge, but during the transition to the afterglow the fluctuations decay away while the axial current in the plasma increases in this very same region. The primary source for driving the fluctuations seems to reside in the temperature and density gradients. Theoretically, the detailed dependence of the growth rate on these gradients depends upon the collisionality of the plasma.

III. SPACE-TIME DEPENDENCE

The spontaneously generated magnetic fluctuations are measured with a small induction-loop probe consisting of mutually orthogonal coils (58 turns of 2.5 mm radius) in a triaxial arrangement. The received signals are filtered with an

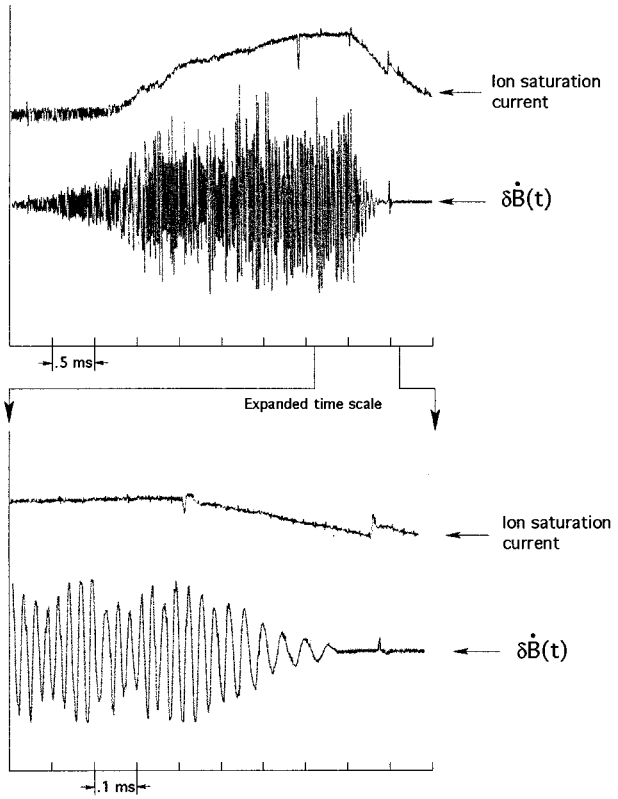

FIG. 6. Temporal development of the magnetic fluctuations and the plasma density. The expanded time scale illustrates the coherency of the magnetic signal and its decay when the discharge is terminated.

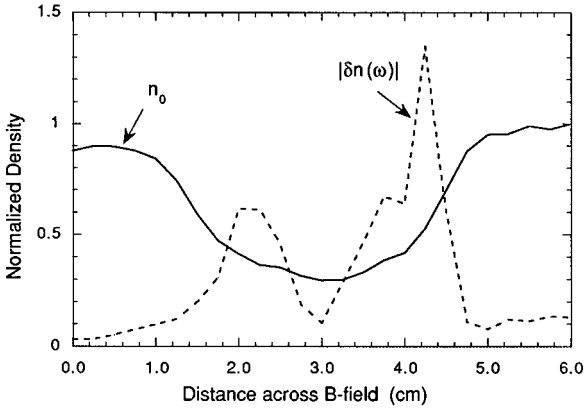

FIG. 7. Radial profile of the Fourier amplitude (linear scale, arbitrary units) of density fluctuations for the frequency corresponding to the peak amplitude (≈37 kHz) superposed on the ion saturation current profile.

RC low-pass filter with the -3 dB point at 1 MHz. The unfiltered probe response varies linearly with frequency from 10 kHz to 1 MHz. The global time evolution of the magnetic noise, $\delta\dot{B}_{\perp}(t)$, detected by this probe in the neighborhood of the striation (at an axial position near the middle of the machine) is exhibited in Fig. 6. The time evolution of the ion saturation current collected by a Langmuir probe is included for reference. The early part of the ion current trace indicates a buildup of plasma density and a subsequent increase in electron temperature. A steady state is obtained and held for about 1 ms after which the discharge current is terminated and a decrease in electron temperature results, as explained in Sec. II. The detected magnetic signal is broadband while the amplitude is growing during the density buildup stage and eventually achieves a steady state consisting of highly coherent low-frequency oscillations, shown in the expanded view at the bottom of Fig. 6, in the range $0.1\ f_{ci}$ ($f_{ci} \equiv \Omega_i/2\pi$). After the discharge current is shut off, the magnetic fluctuations are found to decay while simultaneously decreasing their oscillation frequency. In subsequent discussions of the spectral properties of the fluctuations the time window for the Fourier transform corresponds to the 500 μs interval just prior to termination of the discharge during which steady-state conditions prevail.

Figure 7 displays the spatial dependence of the ambient plasma density, n_0, and the amplitude of the Fourier transform of the density fluctuations $|\delta n(\omega)|$ at a frequency of 37 kHz ($0.085\ f_{ci}$) corresponding to the largest amplitude. For this case the contrast between the density in the center of the striation and the surrounding plasma is about a factor of three. The fluctuations in density are obtained from the local ion saturation current, proportional to $n_0(T_e/M)^{1/2}$, collected by a small Langmuir probe. The local electron temperature is determined from the current-voltage characteristic, but this measurement is not fast enough to be used for correcting the ion saturation current for rapid fluctuations in T_e. Thus the signal we refer to as $|\delta n(\omega)|$ in Fig. 7 also contains contributions arising from fluctuations in the local electron temperature.

It is apparent in Fig. 7 that the density fluctuations are trapped within the striation as would be expected for the radial profile of an eigenmode. The characteristic radial structure exhibits a rough reflection symmetry about the center of the striation and the fluctuation amplitude peaks close to the point where the density gradient is maximum. The fact that the peak Fourier amplitude of the density fluctuation is higher on one side of the striation may be related to asymmetries in the striation density profile introduced by the shaft of the blocking disk. It should be noted, however, that the radial profile shown in Fig. 7 is for the frequency at which the Fourier amplitude is largest. The degree of asymmetry exhibited by the radial profile of the Fourier amplitude depends upon frequency and it is smaller than that exhibited by the profile shown in Fig. 7 at other frequencies.

The radial profile of the amplitude of the Fourier transform of the magnetic field $|\delta B(\omega)|$ at a frequency of 37 kHz is shown in Fig. 8 where the ambient density profile is included for reference as in Fig. 7. The quantity $\delta j_{\parallel}$ also displayed in Fig. 8 is the rms value of the shot-to-shot fluctuations in the axial electric current measured using a double-sided Langmuir probe. The measurements of $|\delta B(\omega)|$ are shown only up to the center of the striation because the shielding and support structure of the magnetic probe is large enough to disturb the shape of the density profile if the probe is inserted through the striation. However, the $\delta j_{\parallel}$ profile is shown across the entire striation because the Langmuir probe is small enough not to significantly disturb the density profile.

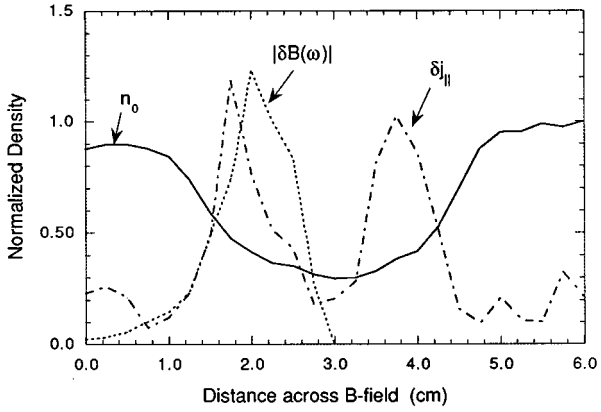

FIG. 8. Radial profiles of fluctuations in the magnetic field-aligned current and the Fourier amplitude (linear scale, arbitrary units) of magnetic field fluctuations superposed on the ion saturation current profile. Only half the magnetic fluctuation profile is shown for reasons given in the text.

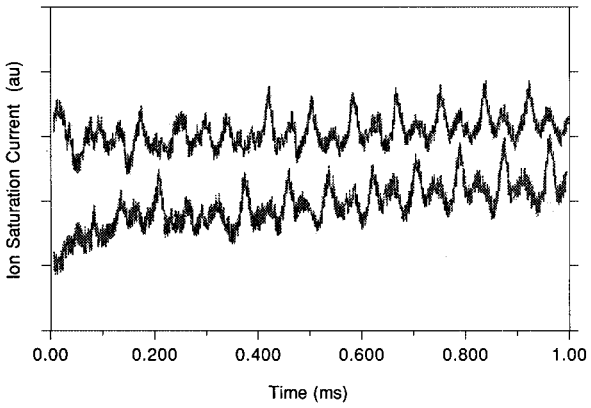

FIG. 10. The temporal behavior of the ion saturation current measured at two diametrically opposed points in the density gradient region of the striation.

The axial variation of the phase of the eigenmode structure is difficult to measure because the wavelength is comparable to or longer than the machine length (i.e., >10 m) while the radial structure varies on a scale of a few mm. Hence it is difficult to ascertain that the probes used for the measurements are aligned within the required precision while simultaneously not perturbing each other (e.g., by plasma shadowing). A more robust method documenting that the radially trapped waves exhibit very weak axial variation consist of a comparison of the frequency spectrum at two well separated axial positions. Figure 9 exhibits the frequency spectrum of density fluctuations obtained with two Langmuir probes at widely separated axial locations, but not inserted simultaneously (i.e., they do not interfere with each other). It is remarkable that most of the spectral features detected within 3 cm of the cathode are reproduced by a probe positioned more than four meters away. Such a behavior can only result if the eigenmodes have very small axial phase variation.

Figure 10 shows the temporal behavior of the ion saturation current measured simultaneously in the density gradient regions on opposite sides of the striation during the later part of the discharge. Large nonsinusoidal density fluctuations are clearly evident. For these particular plasma conditions the density fluctuations exhibit a large fluctuation followed by a smaller fluctuation. The fluctuations on one side of the striation are 180° out of phase with those on the other side. Since the measurement locations are diametrically opposed across the center of the striation this azimuthal variation of the eigenmodes is consistent with an $\exp(i\theta)$ dependence (i.e., $l=1$).

IV. PROPERTIES OF SPECTRA

The polarization of the magnetic fluctuations generated within the striation is extracted from the magnitude of the magnetic flux measured by each of the three mutually orthogonal coils that constitute the magnetic probe. Figure 11 displays the amplitude of the temporal Fourier transform of the fluctuating magnetic field in the direction perpendicular, $|\delta B_{\perp}(\omega)|$, and parallel, $|\delta B_{||}(\omega)|$, to the confining magnetic field at a radial position near the maximum density gradient. It is evident that the magnetic fluctuations are shear waves

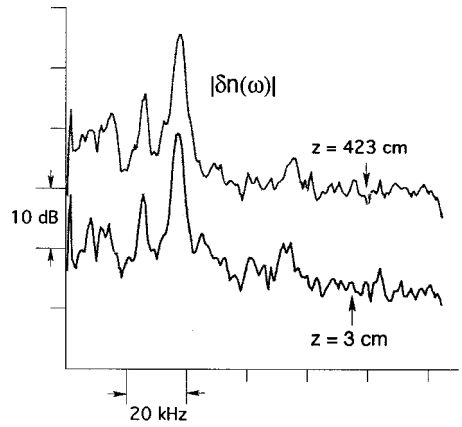

FIG. 9. Frequency spectrum (logarithmic scale) of density fluctuations in the density gradient region of the striation at two axial locations as noted.

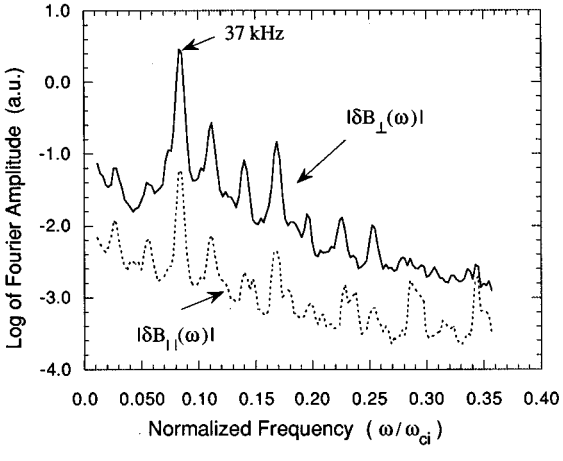

FIG. 11. Frequency spectrum of magnetic field fluctuations perpendicular to the background magnetic field compared to the spectrum of fluctuations parallel to the background field.

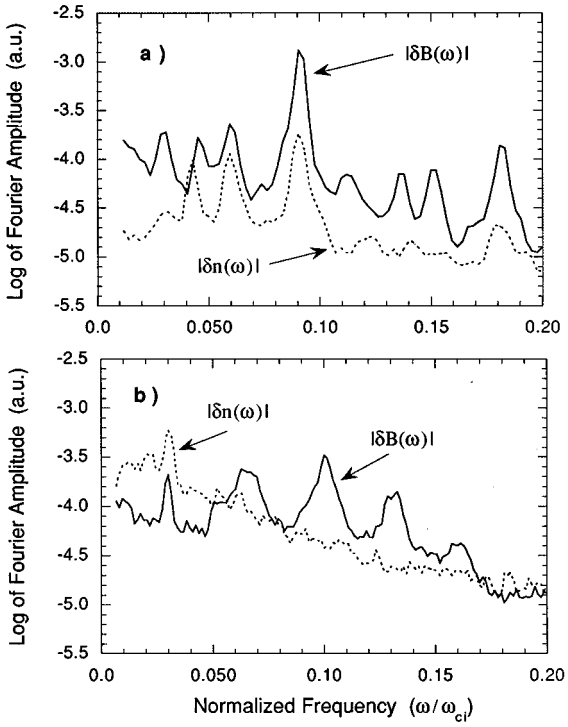

FIG. 12. Frequency spectra of magnetic field fluctuations and density fluctuations for electron beta above the mass ratio (a) and below the mass ratio (b).

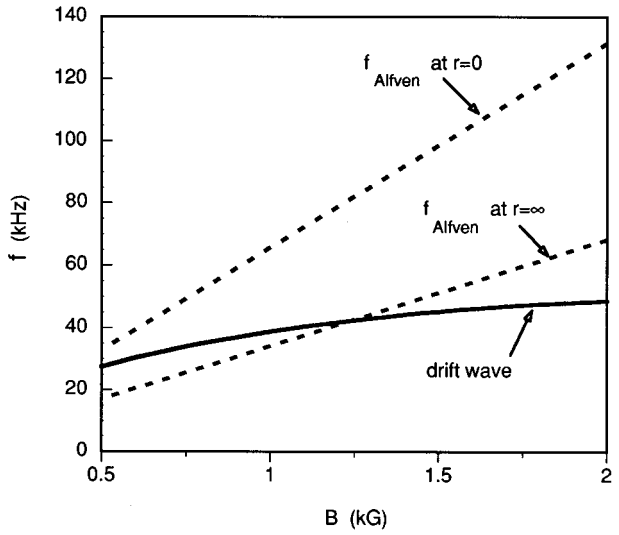

FIG. 13. Theoretical dependence on the strength of the background magnetic field of the frequency of the dominant drift-wave eigenmode (solid curve) and the minimum Alfvén wave frequency inside and outside the striation (dashed curves).

(as opposed to compressional waves), since the parallel component is a factor of 100 times smaller than the perpendicular component. In fact, much of the small parallel component recorded probably results from a slight misalignment of the magnetic probe which results in a portion of the large perpendicular component appearing in the coil purportedly measuring the parallel component.

As already documented in Figs. 7 and 8, radially trapped eigenmodes driven by the gradients can simultaneously exhibit large fluctuations in density and magnetic field. However, the correspondence between density and magnetic eigenmodes does not necessarily hold for all frequencies as the parameters are varied. Figure 12 exhibits the correspondence between $|\delta n(\omega)|$ and $|\delta B(\omega)|$ for two different values of electron plasma beta, β_e. It is seen from Fig. 12(a) that at $\beta_e \approx 10^{-3}$ $(>m/M)$ excellent correspondence is obtained between peaks in the density and magnetic spectra, particularly in the lower range of frequencies $\omega/\Omega_i < 0.1$. In this higher β_e regime it is found from single-shot time traces that the oscillations in density and magnetic field are in phase. Since the magnetic polarization corresponds to shear waves, these modes can be identified as kinetic, drift-Alfvén waves. Figure 12(b) illustrates the behavior obtained as β_e is lowered to 3×10^{-4} $(<m/M)$. It is seen that at this lower beta the correspondence between peaks in the density and magnetic spectra is limited to a small band $\omega/\Omega_i < 0.03$. For these conditions clear peaks exist in the magnetic fluctuations in the region $\omega/\Omega_i > 0.05$ where the density fluctuations exhibit an exponential frequency dependence with no semblance of an eigenmode structure.

Figure 12 illustrates that a separation in the mode structure occurs as the value of β_e is changed. This separation can be understood from the theoretical boundaries shown in Fig. 13. The dashed lines in this figure bound the possible range of frequencies of shear Alfvén modes trapped within a density wave guide corresponding to the experimental parameters; one line corresponds to the Alfvén velocity at the center of the striation and the other to the value in the body of the plasma. As the confining magnetic field is increased the frequency of the pure Alfvén eigenmodes increases, as expected from the linear dependence of the Alfvén speed on magnetic field strength. The solid curve corresponds to the numerically obtained eigenfrequencies of electrostatic drift waves trapped within the striation. Note the correct saturation behavior of the drift-wave eigenfrequencies as the magnetic field is increased. In a semiquantitative sense it is useful to think that the pure drift waves have a frequency related to the familiar local drift frequency

$$\omega_D = \frac{\omega_*}{1+(k_\perp \rho_s)^2}$$

with $k_\perp$ the perpendicular wave number, $\rho_s = (T_e/M)^{1/2}/\Omega_i$, and ω_* the electron diamagnetic drift frequency. Correspondingly the Alfvén eigenmodes approximately satisfy $\omega_A = \pi v_A/L$ where v_A is the Alfvén speed and L the length of the machine. Of course, the proper description requires a rigorous eigenvalue study (the subject of separate publications).

The region in Fig. 13 in which the frequency of the Alfvén modes is smaller than the frequency of the drift waves defines the domain of drift-Alfvén eigenmodes, which for the experimental parameters corresponds to magnetic fields below 1.2 kG, and hence higher β_e. As the magnetic field is increased, and β_e lowered, the pure drift waves have a maximum frequency below 50 kHz, while the pure Alfvén eigenmodes separate and achieve higher frequencies, typically in the range 60–100 kHz. Indeed, the numerical values

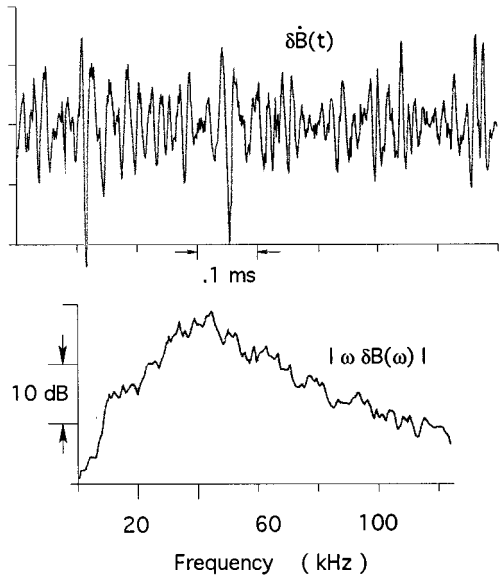

FIG. 14. Single-shot temporal behavior and frequency spectrum (ensemble average) of the time derivative of the magnetic field fluctuations at the outer edge of the plasma column.

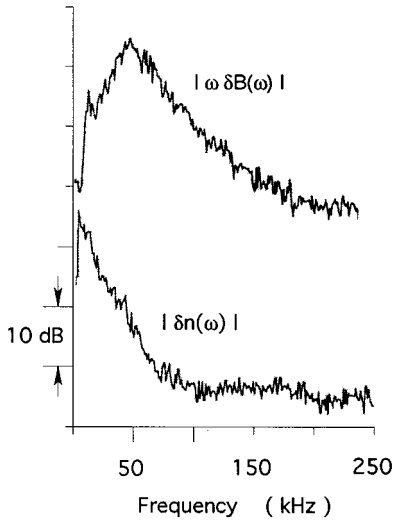

FIG. 15. Frequency spectrum of density fluctuations at the plasma column edge compared to the frequency spectrum of the time derivative of the magnetic field fluctuations (logarithmic scale).

of the spectral peaks shown in Fig. 12 follow this classification. Those in Fig. 12(a) correspond to drift-Alfvén waves, while in Fig. 12(b) the lower band is associated with electrostatic drift waves and the higher frequencies are Alfvén waves.

V. COMPARISON TO EDGE FLUCTUATIONS

The subject of fluctuations driven by edge plasma gradients near a conducting wall has been extensively investigated in the laboratory, primarily in the electrostatic domain accessible to small Q-machine plasma columns,[20–23] and to a more limited extent in tokamak devices[24,25] where both magnetic and density fluctuations are simultaneously present. Small, high-density arcs[26] have also been used to study edge plasma drift-Alfvén waves while global drift-Alfvén waves have been identified[27] in laboratory toroidal devices. Given this background it is natural to compare the properties of fluctuations at the plasma edge and those associated with a filament within the plasma device.

Figure 14 illustrates the typical behavior of the magnetic fluctuations measured at the plasma edge at a position near the maximum density gradient for a discharge current of 2.9 kA and a confining magnetic field of 1.1 kG. The top curve corresponds to the temporal signal of $\delta\dot{B}_{\perp}(t)$ from a single shot and the bottom one to the ensemble averaged spectrum. The temporal signal indicates that the magnetic fluctuations consist of impulsive events followed by a few cycles of clear oscillations. The associated frequency spectrum exhibits a broad peak around 45 kHz (consistent with the lowest frequency of an axial standing shear Alfvén wave) followed by a nearly exponential decay at higher frequencies. The correspondence between the spectrum of magnetic and density fluctuations at the plasma edge is shown in Fig. 15 (over a wider frequency range than used in Fig. 14). The density spectrum peaks toward low frequencies (<10 kHz) and exhibits a clear exponential decay over the frequency range where the magnetic fluctuations have a peak. Clearly, at the plasma edge, the magnetic and electrostatic behavior has separated, in a manner analogous to the fluctuations in the striation at large magnetic fields (i.e., lower β_e). It should be mentioned that by carefully positioning the Langmuir probe at the plasma edge it is possible to identify small peaks that resemble density eigenmodes, but their frequency is generally below 10 kHz and thus well separated from magnetic activity.

In summary, the picture emerging from a study of fluctuations at the plasma edge is that the dominant process consists of impulsive excitation of shear Alfvén waves coexisting with electrostatic drift wave fluctuations with lower frequencies. The broadband nature of the Alfvén turbulence observed at the plasma edge is reminiscent of the situation that develops within the striation at higher magnetic fields, except that within the striation clear signatures of eigenmodes are present as illustrated in Fig. 16.

VI. DISCUSSION

This experimental study has focused on the fluctuations spontaneously generated within a filamentary density depletion whose transverse dimension is on the order of the electron skin depth. Because the region of steep gradients is well separated from external walls and is surrounded by a high-density quiescent plasma, this environment provides a paradigm for the study of gradient driven instabilities because the radial boundary conditions are well-posed. Due to the significant axial extent of the filament an important parameter regime has been examined in which electrostatic drift waves are coupled to shear Alfvén waves resulting in events having simultaneously large fluctuations in density ($|\delta n|/n_0 \approx 0.2$) and magnetic field ($|\delta B|/B_0 \approx 10^{-3}$). Due to the inherent short transverse scale length over which wave activity is gen-

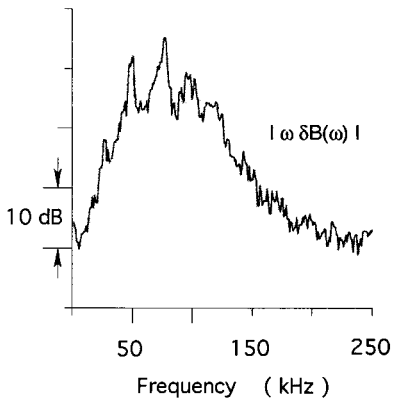

FIG. 16. Frequency spectrum (logarithmic scale) of magnetic fluctuations within the striation at low electron beta (high background magnetic field).

erated, the shear Alfvén waves are not in the regime commonly investigated in global studies (i.e., $k_\perp \to 0$), but instead develop nonzero parallel electric fields. This regime is significant because it provides a mechanism for electron acceleration of relevance to studies of auroral electron beam formation and to models of cross-field energy transport.

Of all the various properties that we have measured, the best theoretical understanding has been achieved in the prediction of the eigenfrequencies and radial eigenmodes of the lower frequency modes that are well approximated by an electrostatic description. An example is given in Fig. 17, in which the solid curves represent analytical results and the open and dark symbols are measured quantities. The predicted frequency of the eigenmode is 38 kHz and the observed value is 37 ± 2 kHz. This theoretical prediction is based on a kinetic description that includes Lorentz collisions for electrons and whose details (too lengthy to be reported here) are the subject of a separate publication. Another feature which is adequately represented by theoretical arguments is the separation of the density and magnetic fluctuations at different values of β_e, as shown in Fig. 12. Overall the measurements are consistent with the criterion $\beta_e \approx m/M$ for the separation between pure drift waves and Alfvén waves.

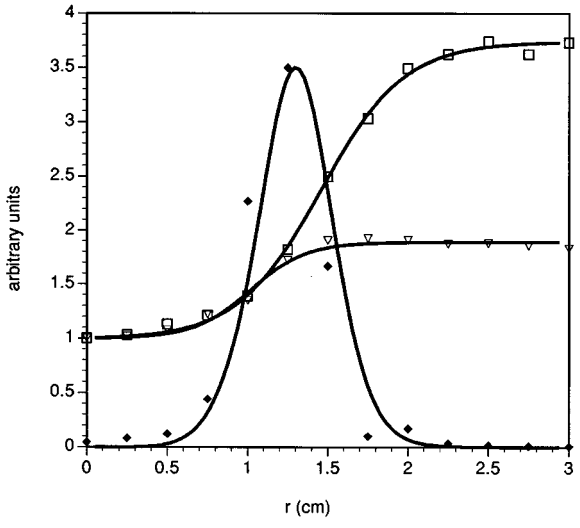

FIG. 17. Theoretical prediction (solid curve) of the radial profile of density fluctuations ($|\delta n|^2$) compared to observed values (solid diamonds). Inverted triangles are measurements of electron temperature and squares are plasma density. Solid curves through these data points represent analytical fits used in the theoretical calculations.

There are several important aspects of the experimental measurements for which we have not yet obtained a satisfactory theoretical understanding and which remain subject to further investigations, both experimental and theoretical. Perhaps the most challenging of these is the description of broadband Alfvén wave turbulence that develops within the striation as the strength of the magnetic field is increased. In particular, since the phenomena develops in the absence of large plasma currents flowing through the striation. A related issue is the possible link between such turbulence and the behavior of the fluctuations observed at the plasma edge at lower magnetic fields. Another important feature which remains to be explained quantitatively is the damping of the eigenmodes after the discharge is terminated.

Although we are not aware of a specific laboratory investigation of fluctuations generated by a microscopic density depletion embedded in a large plasma, an extensive literature exists on the subject of drift instabilities in small plasma columns. Some of these earlier studies share common elements with the present investigation and thus deserve explicit comparison. The pioneering experiment[26] of Tang and Luhmann (TL) identified the existence of drift-Alfvén waves in a high density arc jet in which the density gradient scale length was an order of magnitude larger than the electron skin depth, i.e., in the parameter regime $L_n \approx \rho_i \gg c/\omega_{pe}$. Although no magnetic and density radial eigenfunctions were measured, evidence was presented that the modes had both density and magnetic fluctuations, of the type we observe at higher β_e ($> m/M$). TL used a field-aligned plasma current to excite a pure Alfvén wave at frequencies larger than the mode identified as the drift-Alfvén wave. The reported value of the current, however, was not consistent with the parameters quoted. Although a small broadening of the spectrum of the current-driven Alfvén wave was observed, the regime of broadband Alfvén wave turbulence sampled in our study at lower β_e ($< m/M$) was not achieved. In summary, the features of the low frequency mode studied by TL are reminiscent of the behavior sampled in our experiment at the plasma edge, but the broadband Alfvén wave turbulence simultaneously present is quite different. This behavior may arise because the perpendicular wavelength of the structures in our experiment are comparable to the electron skin depth.

Drift-Alfvén waves have also been investigated by Fredrickson and Bellan[27] (FB) in a toroidal device operated at low magnetic field in a parameter regime close to that of TL, namely, $L_n \approx \rho_i/3 \gg c/\omega_{pe}$. The eigenmodes observed were of a global type with the density and magnetic fluctuations showing significantly different radial structures. This is in contrast to our observations of highly peaked eigenfunctions in which the density and magnetic patterns are quite similar. This difference in observed behavior may be related to the microscopic dimension of the striation in our study. The transition to pure Alfvén waves seen in our experiment and

also sampled in the study by TL were not reported by BF. In addition, BF make no reference to exponential spectra at the plasma edge, as is seen in our experiment and also reported by Fiksel *et al.*[25]

No clear indication of the damping mechanism of drift-Alfvén waves was documented in the work of TL and FB. A mechanism frequently included in theoretical descriptions of these modes is ion viscosity. However, no direct experimental confirmation of the process has been documented, including this study. In an ingenious experiment in a Q-machine plasma Barrett and Allen[28] (BA) attempted to document the damping mechanism of electrostatic drift-waves driven unstable by a pulsed annular beam of slow electrons. BA concluded that ion viscosity was not sufficient to explain their measurements, but that the ion transit time along the column, a mechanism previously invoked by Rowberg and Wong,[29] played an important role. The concensus appears to be that there is an active mechanism responsible for the damping of drift-Alfvén waves in laboratory plasmas which is not included in the standard theoretical treatments. Our observations corroborate this perspective.

The role of a radial electric field on the stability of electrostatic drift-waves in a small plasma column dominated by neutral collisions has been investigated by Marshall *et al.*[30] The measured radial eigenfunctions were highly localized at the plasma edge and exhibited a similarity to the shape of the radially trapped eigenmodes in our experiment. Marshall *et al.* concluded that the radial electric field generated by drawing a current through a grid intersecting their plasma was responsible for driving the instability. Although radial electric fields were intrinsically present in the TL experiment, no significant features were attributed to the resulting rotation. Similarly in our experiment, some fine details not reported here could be related to shear in azimuthal rotation within the striation, however, the numerical values of the eigenfrequencies are well-explained by the inclusion of the diamagnetic drifts alone, as is also the case in TL and BF. An intriguing possibility raised by the study of Marshall *et al.* is that the decay we observe after the discharge current is shut off may be related to the radial electric field. Clearly, a more detailed study focused on this effect is warranted.

It should be emphasized that in our experiment we clearly identify exponential dependencies of the density spectra at the plasma edge and, under some conditions, also within the striation. Similar exponential behavior has been observed in tokamak geometry by Fiksel *et al.*[25] Thus, it must be concluded that this exponential character is a universal feature unrelated to any peculiarities of tokamak dynamics, as is also corroborated by observations in a linear device at low magnetic fields by Kauschke *et al.*[31]

A noteworthy result of our experiment is that the growth of the density and magnetic fluctuations does not destroy the striation over a length along the confining magnetic field of over 10^6 Debye lengths. Thus, if a similar process is occurring in the auroral ionosphere, one might expect to find density striations filled with relatively time-steady magnetic fluctuations with frequencies lower than the gyrofrequency of the majority ion species. In this regard it is interesting to note that Alfvén waves have been associated[32] with regions of auroral electron precipitation and that the Alfvén speed at altitudes on the order of one Earth radius corresponds to the velocity of keV electrons. Furthermore, the largest parallel electric fields should be associated with cross-field lengths on the size of the electron skin depth which scales very well with the thickness of discrete auroral arcs.[33]

ACKNOWLEDGMENTS

We thank Professor W. Gekelman and D. Leneman for valuable contributions to this experiment. Results of theoretical studies reported here have been done in collaboration with J. Peñano.

This work is sponsored by the Office of Naval Research and the National Science Foundation.

[1] J. B. Taylor, Phys. Fluids B **5**, 4378 (1993).
[2] J. F. Drake, R. G. Kleva, and M. E. Mandt, Phys. Rev. Lett. **73**, 1251 (1994).
[3] R. G. Kleva, Phys. Rev. Lett. **73**, 1509 (1994).
[4] R. Kinney, T. Tajima, J. C. McWilliams, and N. Petviashvili, Phys. Plasmas **1**, 260 (1994).
[5] S. J. Zweben and S. S. Medley, Phys. Fluids B **1**, 2058 (1989).
[6] N. J. Lopes Cardozo, F. C. Schuller, C. J. Barth, C. C. Chu, F. J. Pipjer, J. Lok, and A. A. M. Oomens, Phys. Rev. Lett. **73**, 256 (1994).
[7] G. Castle, Ph.D. dissertation, University of Texas, Austin, 1994.
[8] M. C. Kelley, T. L. Arce, J. Salowey, M. Sulzer, W. T. Armstrong, M. Carter, and L. Duncan, J. Geophys. Res. **100**, 17367 (1995).
[9] P. M. Kintner, J. Vago, S. Chesney, R. L. Arnoldy, K. A. Lynch, C. J. Pollock, and T. E. Moore, Phys. Rev. Lett. **68**, 2448 (1992).
[10] A. I. Eriksson, B. Holback, P. O. Dovner, R. Bostrom, G. Homgren, M. André, L. Eliasson, and P. M. Kintner, Geophys. Res. Lett. **21**, 1843 (1994).
[11] C. G. Durfee III and H. M. Milchberg, Phys. Rev. Lett. **71**, 2409 (1993).
[12] G. J. Morales, R. S. Loritsch, and J. E. Maggs, Phys. Plasmas **1**, 3775 (1994).
[13] W. Gekelman, D. Leneman, J. Maggs, and S. Vincena, Phys. Plasmas **1**, 3775 (1994).
[14] T. Ohkawa, Phys. Lett. A **67**, 35 (1978).
[15] G. J. Morales and H. Ramachandran, *International Conference on Plasma Physics*, Innsbruck, 1992 (European Physical Society, Petit-Lancy, 1992), Vol. 16 C, p. I-135.
[16] A. Hasegawa, J. Geophys. Res. **81**, 5083 (1976).
[17] J. M. McChesney, P. M. Bellan, and R. A. Stern, Phys. Fluids B **3**, 3363 (1991).
[18] G. Gustafsson, M. André, L. Matson, and H. Koskinen, J. Geophys. Res. **95**, 5889 (1990).
[19] W. Gekelman, H. Pfister, Z. Lucky, J. Bamber, D. Leneman, and J. Maggs, Rev. Sci. Instrum. **62**, 2875 (1991).
[20] H. Lashinsky, Phys. Rev. Lett. **12**, 121 (1964).
[21] H. W. Hendel, T. K. Chu, and P. A. Politzer, Phys. Fluids **11**, 2426 (1968).
[22] P. A. Politzer, Phys. Fluids **14**, 2410 (1971).
[23] R. F. Ellis and R. W. Motley, Phys. Fluids **17**, 582 (1974).
[24] S. J. Zweben and R. J. Taylor, Nucl. Fusion **21**, 193 (1981).
[25] G. Fiksel, S. C. Prager, P. Pribyl, R. J. Taylor, and G. R. Tynan, Phys. Rev. Lett. **75**, 3866 (1995).
[26] J. T. Tang and N. C. Luhmann, Jr., Phys. Fluids **19**, 1935 (1976).
[27] E. D. Fredrickson and P. M. Bellan, Phys. Fluids **28**, 1866 (1985).
[28] P. J. Barrett and G. R. Allen, Phys. Fluids **26**, 795 (1983).
[29] R. E. Rowberg and A. Y. Wong, Phys. Fluids **13**, 661 (1970).
[30] E. Marden Marshall, R. F. Ellis, and J. E. Walsh, Plasma Phys. Controlled Fusion **28**, 1461 (1986).
[31] U. Kauschke, G. Oelerich-Hill, and A. Piel, Phys. Fluids B **2**, 38 (1990).
[32] M. H. Boehm, C. W. Carlson, J. P. McFadden, J. H. Clemmons, and F. S. Mozer, J. Geophys. Res. **95**, 12157 (1990).
[33] J. E. Borovsky, J. Geophys. Res. **98**, 6101 (1993).